THE JOURNAL OF BIOLOGICAL CHEMISTRY VOL. 292, NO. 12, pp. 5110–5122, March 24, 2017

Novel Interconnections in Lipid Metabolism Revealed by Overexpression of Sphingomyelin Synthase-1*

Received for publication, August 8, 2016, and in revised form, January 13, 2017 Published, JBC Papers in Press, January 13, 2017, DOI 10.1074/jbc.M116.751602

Gergana M. Deevska[‡], Patrick P. Dotson II[‡], Alexander A. Karakashian[‡], Giorgis Isaac[§], Mark Wrona[§], Samuel B. Kelly[¶], Alfred H. Merrill, Jr.[¶], and Mariana N. Nikolova-Karakashian[‡1]

From the [‡]Department of Physiology, University of Kentucky, Lexington, Kentucky 40536, [§]Pharmaceutical Discovery and Life Sciences, Waters Corporation, Milford, Massachusetts 01757, and the [¶]School of Biology and Petit Institute for Bioengineering and Bioscience, Georgia Institute of Technology, Atlanta, Georgia 30332

Edited by George M. Carman

This study investigates the consequences of elevating sphingomyelin synthase 1 (SMS1) activity, which generates the main mammalian sphingolipid, sphingomyelin. HepG2 cells stably transfected with SMS1 (HepG2-SMS1) exhibit elevated enzyme activity *in vitro* and increased sphingomyelin content (mainly C22:0- and C24:0-sphingomyelin) but lower hexosylceramide (Hex-Cer) levels. HepG2-SMS1 cells have fewer triacylglycerols than controls but similar diacylglycerol acyltransferase activity, triacylglycerol secretion, and mitochondrial function. Treatment with 1 mM palmitate increases *de novo* ceramide synthesis in both cell lines to a similar degree, causing accumulation of C16:0-ceramide (and some C18:0-, C20:0-, and C22:0-ceramides) as well as C16:0- and C18:0-Hex-Cers. In these experiments, the palmitic acid is delivered as a complex with delipidated BSA (2:1, mol/mol) and does not induce significant lipotoxicity. Based on precursor labeling, the flux through SM synthase also increases, which is exacerbated in HepG2-SMS1 cells. In contrast, palmitate-induced lipid droplet formation is significantly reduced in HepG2-SMS1 cells. [^{14}C]Choline and [^{3}H]palmitate tracking shows that SMS1 overexpression apparently affects the partitioning of palmitate-enriched diacylglycerol between the phosphatidylcholine and triacylglycerol pathways, to the benefit of the former. Furthermore, triacylglycerols from HepG2-SMS1 cells are enriched in polyunsaturated fatty acids, which is indicative of active remodeling. Together, these results delineate novel metabolic interactions between glycerolipids and sphingolipids.

The sphingomyelin synthase (SMS)[2] generates the main mammalian sphingolipid, sphingomyelin (SM), by transferring a phosphocholine group from phosphatidylcholine (PC) to ceramide and in the process produces diacylglycerols (DGs) (1, 2). Thus, SMS controls the homeostasis of two key bioactive lipids, ceramide and DG, and presents a point of convergence for glycerolipid and sphingolipid metabolism.

Sphingolipids are a class of lipid molecules characterized by the presence of an 18-carbon aliphatic chain called a sphingoid base. Sphingosine and sphinganine are the main sphingoid bases in mammalian cells. Sphinganine, a precursor for most mammalian sphingolipids, is produced in the endoplasmic reticulum (ER) from L-serine and palmitoyl-CoA by the action of serine palmitoyltransferase (SPT). Sphinganine is then acylated by ceramide synthases, a family of six acyltransferases with distinct specificity for acyl-CoAs of particular chain lengths, to form dihydroceramide. With the desaturation of the 4,5-carbon bond in the sphingoid base, dihydroceramide is converted to ceramide (3) and then transferred from the ER to the Golgi (4), where phosphorylcholine or a glucose group is added to the primary hydroxyl of ceramide to produce SM or glucosylceramide.

Glycerolipids, in turn, are structurally and metabolically a distinct class of lipids, the synthesis of which begins with the acylation of glycerol 3-phosphate with two acyl-CoA molecules to form 1,2-diacylglycerol phosphate (phosphatidic acid). The phosphate is then removed, generating DG, a key intermediate in several lipid metabolic pathways. The acylation of DG by acyl-CoA:diacylglycerol acyltransferase (DGAT) leads to the formation of triacylglycerols (TG) (5–7). Alternatively, the addition of a phosphobase (from CDP-choline or CDP-ethanolamine) to DG by the choline/ethanolamine phosphotransferase 1 (CEPT1) produces PC or phosphatidylethanolamine (PE), the two main glycerophospholipids. There is evidence suggesting that TG and phospholipid synthesis pathways utilize a common pool of DG in a competitive manner. Decreased incorporation of DG into TG, for example, is observed in proliferating cells that have an increased necessity for phospholipids for mem-

* This work was supported by National Institutes of Health (NIH) Grant R01AG019223 (to M. N. K.), American Heart Association (AHA) Postdoctoral Fellowship 11POST7650060 (to G. D.), AHA Postdoctoral Fellowship 10POST4300013 (to P. D.), and NIH Grant R01GM076217 (to A. H. M.). The authors declare that they have no conflicts of interest with the contents of this article. The content is solely the responsibility of the authors and does not necessarily represent the official views of the National Institutes of Health.

[1] To whom correspondence should be addressed: MS513, Chandler Medical Center, 800 Rose St., Lexington, KY 40536. Tel.: 859-323-8210; Fax: 859-323-1070; E-mail: mariana.karakashian@uky.edu.

[2] The abbreviations used are: SMS, sphingomyelin synthase; CCT1, CTP:phosphocholine cytidylyltransferase 1; CEPT1, choline/ethanolamine phosphotransferase 1; DG, diacylglycerol; DGAT, diacylglycerol acyltransferase; EV, empty vector; ER, endoplasmic reticulum; GCS, glucosylceramide synthase; Hex-Cer; hexosylceramide; NBD-Cer, *N*-hexanoyl-((*N*-(7-nitrobenz-2-oxa-1,3-diazol-4-yl)amino)-sphingosine; NBD-SM, *N*-hexanoyl-sphingosine-1-phosphocholine; OCR, oxygen consumption rate; OPLS-DA, orthogonal partial least squares-discriminant analysis; PC, phosphatidylcholine; PDMP, 1-phenyl-2-decanoyl amino-3-morpholino-1-propanol; PE, phosphatidylethanolamine; PS, phosphatidylserine; SM, sphingomyelin; SPT, serine-palmitoyltransferase; TG, triacylglycerol(s); FCCP, carbonyl cyanide *p*-trifluoromethoxyphenylhydrazone; MEM, minimum essential medium.

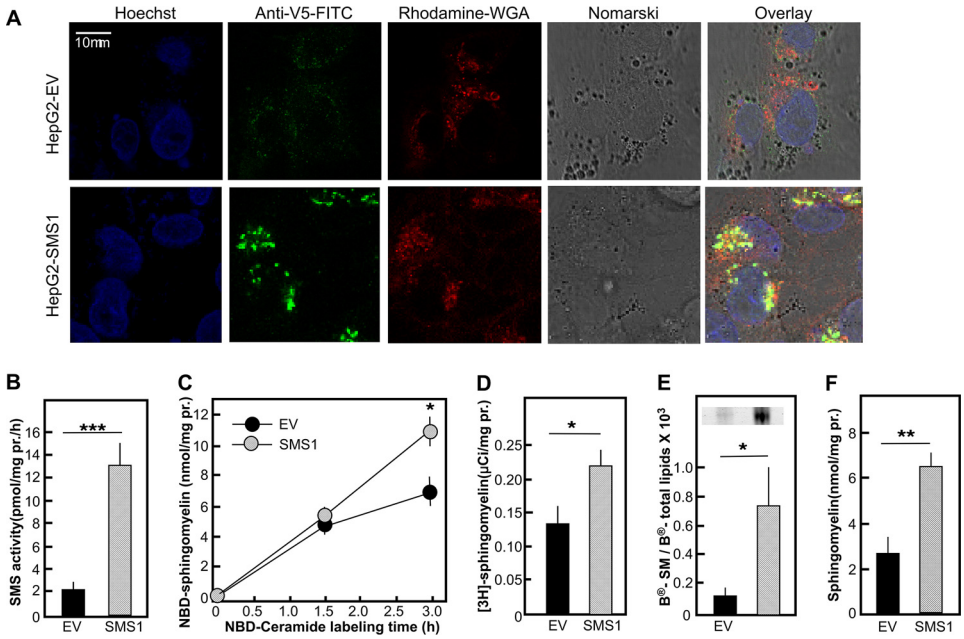

FIGURE 1. **Characterization of SMS1 protein expression and activity in HepG2 cells.** The HepG2-SMS1 cell line stably overexpresses the human V5-tagged SMS1 (HepG2-SMS1), whereas HepG2-EV is the empty vector control cell line. *A*, expression and subcellular localization of the V5-tagged SMS1 protein (*green*) visualized by indirect immunofluorescence in permeabilized cells using antibody against the V5 tag. Hoechst 33258 (*blue*) and wheat germ agglutinin (*WGA*; *red*) were used for staining of the nuclei and Golgi. *B*, SM synthase activity measured *in vitro*. *C–E*, *in situ* labeling of SM in live cells using NBD-ceramide (*C*), [^{3}H]palmitic acid (*D*), and BODIPY®-palmitic acid (*E*) as tracers. *F*, mass of SM measured by TLC separation of total lipid extract and quantification of inorganic phosphate. Mean values ± S.D. (*error bars*) are shown ($n = 3$ dishes/point). Results were confirmed in at least three independent experiments, and representative data are shown. *, $p < 0.05$; **, $p < 0.01$; ***, $p < 0.001$ according to Student's *t* test.

brane formation (8). Also, the direct inhibition of CEPT1 or the genetic deletion of phosphoethanolamine cytidylyltransferase, which catalyzes the formation of CDP-ethanolamine for PE synthesis, has been shown to stimulate the synthesis of TG by as much as 10-fold (8, 9). The overexpression of DGAT1, on the other hand, has been shown to inhibit the synthesis of glycerophospholipids (10).

Despite the fact that SMS activity also influences DG homeostasis in the cells, the impact it has on glycerolipid metabolism is unknown. Several studies in mice indicate that the rate of SM synthesis influences TG synthesis and/or degradation (11, 12). High fat diet-induced accumulation of TG in the liver, for example, was substantially reduced in the acid sphingomyelinase knock-out mouse model, where stimulation of sphingolipid synthesis was exacerbated by the disruption of the negative feedback regulatory mechanisms (11). In contrast, reduction in hepatic SM levels was found to correlate with increased TG accumulation (12).

SM synthase exists in two isoforms: the Golgi-localized SMS1 and the plasma membrane-associated SMS2. To directly test the relationship between SMS1 and glycerolipid synthesis, we stably overexpressed SMS1 in HepG2 cells. We show that HepG2-SMS1 cells exhibit an attenuated rate of TG synthesis, especially in the presence of excess palmitic acid. The chronic up-regulation of SMS1 activity appears to activate PC depletion-sensing mechanisms at the Golgi and to stimulate the Kennedy pathway of *de novo* PC synthesis, thus diverting DG precursors away from DGAT and TG synthesis.

Results

HepG2-SMS1 Cells Produce Functionally Active SMS1—The full-length human V5-tagged SMS1 was stably transfected in HepG2 cells, creating the HepG2-SMS1 cell line. Similarly, the empty vector was used to make the HepG2-EV control cell line. Indirect immunofluorescence confirmed that SMS1 was overexpressed and that the protein co-localized with the Golgi marker WGA (Fig. 1*A*). To determine whether the protein was functionally active, *in vitro* enzymatic activity assay and *in situ* labeling studies were done. The SMS1-overexpressing cells had 6-fold higher SMS activity than the HepG2-EV cells (Fig. 1*B*). Labeling experiments with NBD-ceramide and with ^{3}H- or BODIPY®-labeled palmitic acid (precursor for the *de novo* sphingolipid biosynthesis) also showed that HepG2-SMS1 cells have elevated synthesis of SM (Fig. 1, *C–E*). The SMS1-overexpressing cells also had higher levels of SM, as compared with the control cells, based on quantification of the total inorganic phosphate following TLC separation (Fig. 1*F*). Surprisingly, the levels of ceramide were similar in the two cell lines (data not shown).

SMS1 Overexpression in Hepatic Cells Affects Hexosylceramide (Hex-Cer) Homeostasis—To obtain a more comprehensive picture of the changes in sphingolipid homeostasis evoked by SMS1 overexpression, a mass spectrometry-based analysis of SM, ceramide, and Hex-Cer was done. Several SM species followed a trend of increase (Fig. 2*A*), but only for C22:0- and C24:0-SM were the differences statistically significant. It should be noted that liver produces mainly sphingolipids with C22 and C24 chain lengths because of the high levels of Cers2 expression. With regard to Hex-Cer levels, the C18:1, C20:0, C26:0, C16:0, and C24:1 were significantly lower in HepG2-SMS1 cells (Fig. 2*B*).

In situ labeling with NBD-ceramide, which is known to localize to the Golgi, indicated that there is a competition for avail-

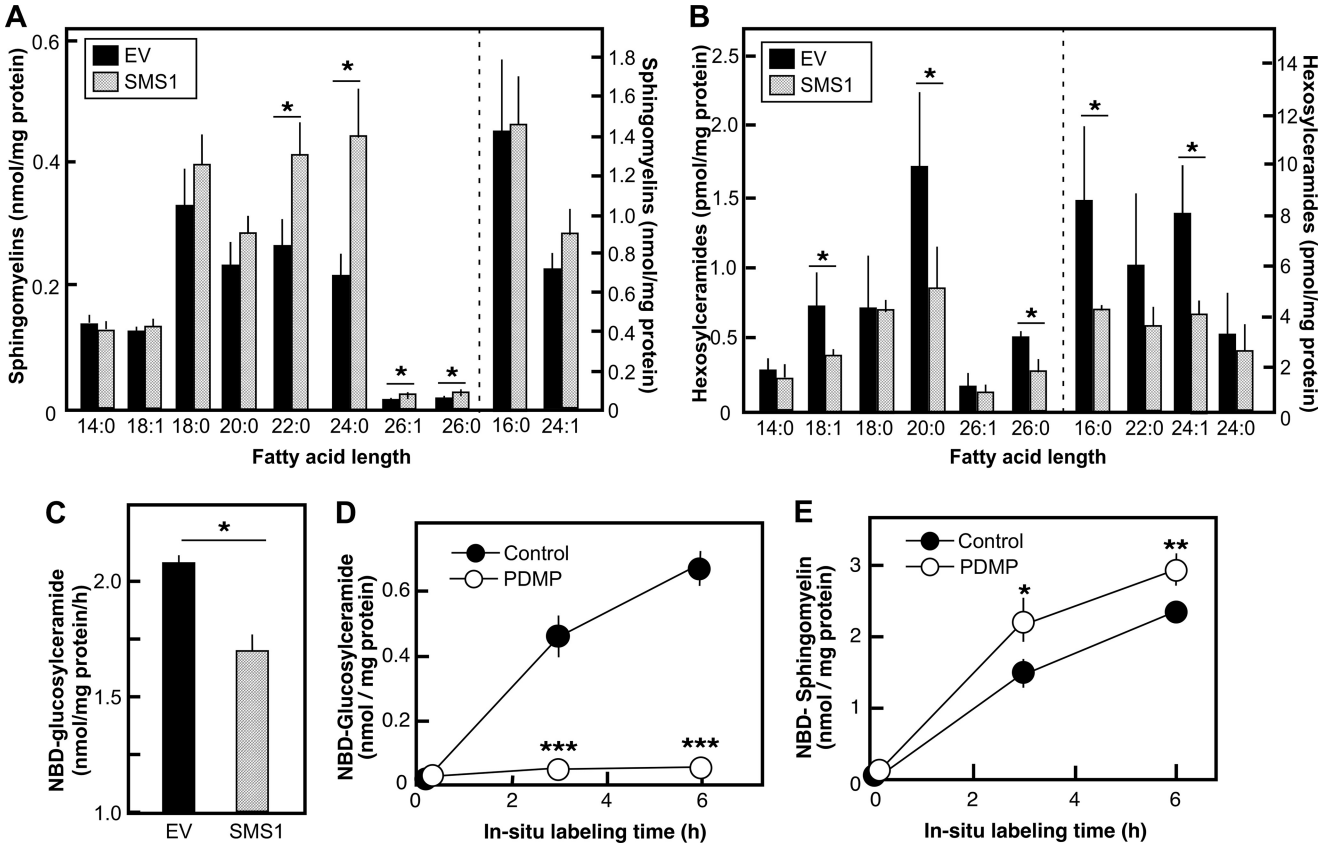

FIGURE 2. **Effect of SMS1 overexpression on SM and Hex-Cer levels and synthesis.** *A* and *B*, quantification of sphingomyelin (*A*) and hexosylceramide (*B*) species in total lipid extracts of HepG2-SMS1 and control cells by mass spectrometry. *C*, NBD-ceramide incorporation into glucosylceramide in control and SMS1-overexpressing cells. *D* and *E*, effects of GCS inhibition using PDMP on the formation of NBD-glucosylceramide and NBD-SM. PDMP (25 μM) was added 1 h before the addition of NBD-ceramide, and cells were harvested at the indicated time points. Conversion of NBD-Cer to NBD-glucosylceramide or NBD-SM was quantified using HPLC. Data are shown as mean values ± S.D. (*error bars*) ($n = 3$ dishes/point). *, $p < 0.05$; **, $p < 0.01$; ***, $p < 0.001$ according to Student's *t* test. Results were confirmed in two independent experiments.

able ceramide between the SMS1 and GCS. As seen in Fig. 2*C*, HepG2-SMS1 cells produced less NBD-glucosylceramide than the control cells (Fig. 2*C*). Treatment of HepG2-SMS1 cells with PDMP, a GCS inhibitor, blocked the formation of NBD-glucosylceramide and increased the incorporation of the label into NBD-SM (Fig. 2, *D* and *E*). Hence, SMS1 utilizes, at least in part, the same pool of ceramide, as does GCS. These results also suggest that the ceramide levels in the Golgi may be a rate-limiting factor for SM synthesis.

Treatment with Palmitic Acid Leads to Increased Levels of Ceramide and Hex-Cer—To increase the availability of ceramide in the cells we added palmitic acid, which is known to stimulate the *de novo* ceramide synthesis (13). The palmitate was supplemented at 1 mM final concentration. Following treatment, cell viability was >90% at 18 h, indicating that palmitate-associated toxicity was relatively low. As anticipated, the palmitate treatment increased most ceramide species by 25–50%, whereas C16:0-ceramide increased almost 100% (Fig. 3*A*). This widespread effect is consistent with stimulation of SPT activity. The augmented response seen in C16-ceramide levels probably reflects the increased abundance of C16-palmitic acid in the overall pool of fatty acids available for the ceramide synthases (especially for CerS6, which has a preference for C16 palmitic acid).

Next, we examined how palmitate addition affects the levels of Hex-Cer (Fig. 3*C*) and SM (Fig. 3*B*). C16:0 Hex-Cer (and to a lesser extent C18:0 Hex-Cer) increased, whereas C20:0- and C22:0-Hex-Cer were not affected despite the observed elevated abundance of the respective ceramide precursors. None of the examined SM species increased following the palmitate treatment. SMS1 overexpression did not alter the palmitic acid effects on ceramide, Hex-Cer, and SM (data not shown). It should be pointed out, however, that even for C16-ceramide, the most abundant of all ceramide species, the amplitude of palmitate-induced change was around 400 pmol/mg protein, which is within the standard deviation of the measurement of the respective C16-SM (±300 pmol/mg protein). Therefore, mass measurements may have limited power in detecting palmitate-induced changes in SM because of the high basal levels of that lipid.

As an alternative approach, we compared the incorporation of [^{3}H]palmitic acid into ceramide and SM at low (0.1 mM) and high (1 mM) palmitate concentrations, delivered at a constant specific labeling. The labeling of ceramide in cells treated with 1 mM [^{3}H]palmitic acid was 15 times higher than in cells treated with 0.1 mM [^{3}H]palmitate (*i.e.* 0.789 μCi/mg protein *versus* 0.050 μCi/mg protein). This confirms the potent stimulatory effects of palmitate on SPT and the *de novo* ceramide synthesis.

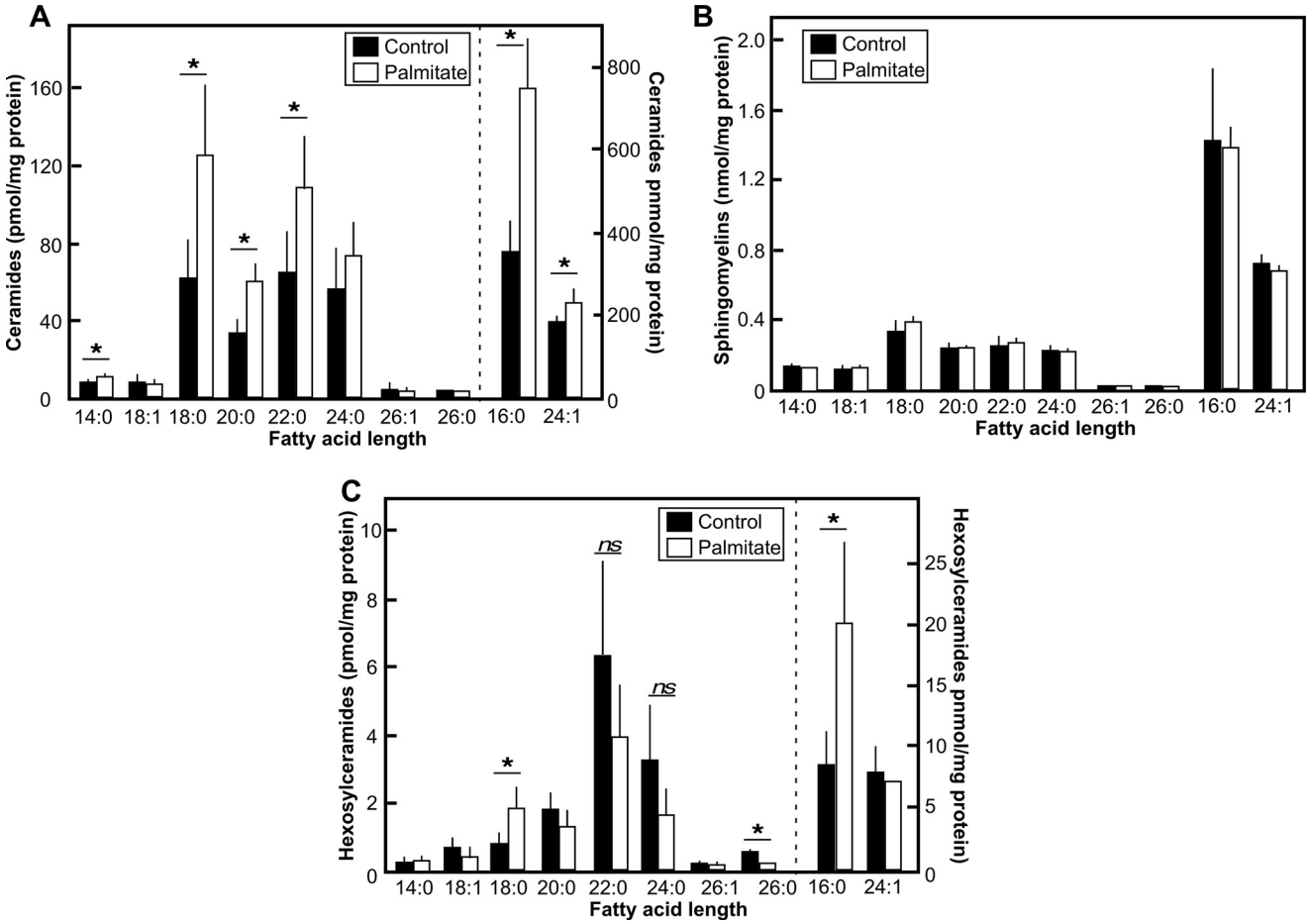

FIGURE 3. **Effect of palmitic acid on the levels of different sphingolipids.** HepG2 cells were cultured for 18 h in the presence of either 1 mM palmitic acid delivered as a BSA complex (2:1, mol/mol) or 0.5 mM BSA as a vehicle control. Total lipid extracts were prepared, and ceramide (*A*), SM (*B*), and Hex-Cer (*C*) species were measured by mass spectrometry. Data are shown as mean values ± S.D. (*error bars*) ($n = 3$ dishes/point). *, $p < 0.05$ according to Student's *t* test. Results were confirmed in two independent experiments.

Statistically significant increases were also seen for SM, although these increases were somewhat smaller in magnitude (*i.e.* 0.339 μCi/mg protein *versus* 0.130 μCi/mg protein, a 3-fold difference).

Together, these data indicate that palmitate supplementation stimulates *de novo* synthesis and accumulation of ceramide. A portion of the newly synthesized ceramide can be effectively converted to glucosylceramide and SM, although a net increase in mass could be detected only for the former.

SMS1 Overexpression Affects the Ability of Cells to Accumulate TG—In hepatocytes, elevated fatty acid supply is known to result in the formation of lipid droplets containing TG. We used Oil Red-O (a fat-soluble dye that stains neutral lipids like TG and esterified cholesterol) to visualize lipid droplet formation in HepG2-EV and HepG2-SMS1 cells. The control cells were seen to contain some lipid droplets, even in the absence of palmitate. As expected, the abundance of these lipid droplets increased substantially after overnight incubation with 1 mM palmitic acid (Fig. 4*A*). The HepG2-SMS1 cells, however, were virtually devoid of any stained droplets and even after incubation with 1 mM palmitic acid had very few Oil Red-O-positive droplets, as compared with the control cells (Fig. 4*A*). Measurement of TG mass confirmed these differences in the TG accumulation (Fig. 4*B*). Notably, the effects were TG-specific, because the levels of total cholesterol (free and esterified) were similar in the two cell lines (Fig. 4*C*).

To eliminate the possibility that these observations were an artifact of the stable transfection, similar experiments were performed in HepG2 cells transiently transfected with the overexpressing SMS1 construct. Western blotting analysis with anti-V5 antibody confirmed overexpression of the V5-tagged SMS1 (data not shown). This overexpression led to increased SMS activity, as judged by the increased conversion of radiolabeled [^{3}H]palmitic acid into SM (Fig. 4*D*) in SMS1-overexpressing cells, and the effect was greater in cells treated with 1 mM palmitic acid. As seen with the stably transfected cells, palmitate incorporation into TG in SMS1-overexpressing cells was diminished both at the basal state and after treatment with 1 mM palmitic acid (Fig. 4, *E* and *F*).

Decreased TG Accumulation in HepG2-SMS1 Cells Is Not Due to Impaired DGAT Activity or Increased Fat Export—Next, we sought to identify the mechanism(s) responsible for the diminished TG accumulation seen in HepG2-SMS1 cells. Labeling experiments using BODIPY-palmitic acid (Fig. 5*A*) confirmed that these cells have reduced incorporation of the precursor into TG. To further explore more directly the effects on the rate of TG synthesis, we assessed the activity of DGAT in live cells using radioactive acyl-CoA as a donor, exogenously

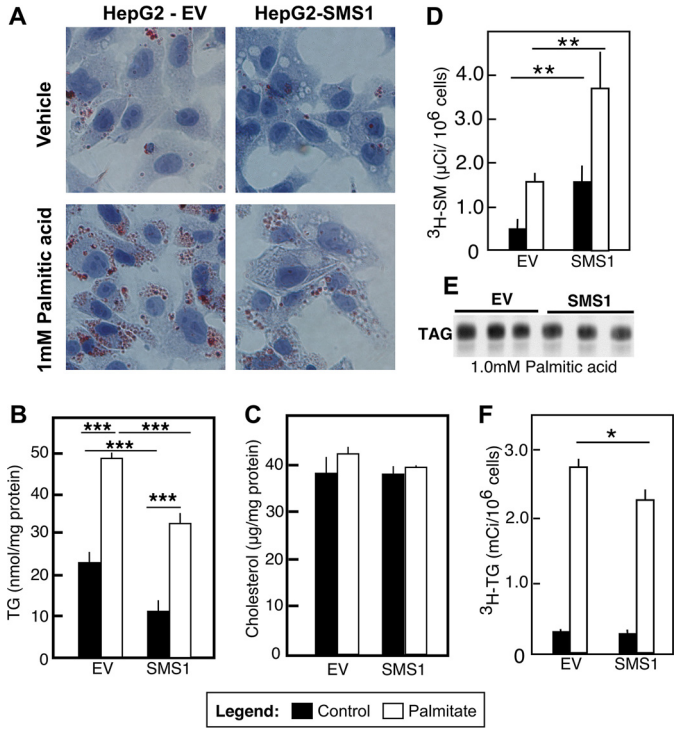

FIGURE 4. **SMS1 overexpression attenuates the ability of cells to accumulate TG.** *A–C*, HepG2-SMS1 and HepG2-EV cells were incubated with 1 mM palmitic acid delivered as a BSA complex (2:1, mol/mol) or with vehicle control (0.5 mM BSA) for 18 h**.** *A*, formation of lipid droplets visualized by Oil Red-O staining. *B* and *C*, levels of TG (*B*) and total cholesterol (*C*) measured in total lipid extracts as described under "Experimental Procedures." Mean values ± S.D. (*error bars*) are shown ($n = 3$ dishes/point). *D–F*, HepG2 cells transiently transfected with SMS1 or EV were incubated with 0.1 or 1 mM ^{3}H-labeled palmitic acid for 18 h. The specific labeling in each case was kept at 50 mCi/mmol. Lipids were extracted and separated by TLC as described under "Experimental Procedures." *D*, radioactivity from the bands corresponding to SM quantified by scintillation counting. *E*, representative scan for ^{3}H-labeled TG at 1 mM palmitic acid. *F*, radioactivity associated with TG determined by scintillation counting. According to two-way analysis of variance, the main effects of palmitate treatment and SMS1 overexpression on TG were statistically significant. The interaction effect was not statistically significant. The results of Bonferroni post-test analyses are indicated (***, $p < 0.001$; **, $p < 0.01$; *, $p < 0.05$). Results were confirmed in at least four independent experiments.

added DG as an acceptor substrate, and a permeabilization procedure that allowed for the quantification of the overt (associated with the cytosol) and latent (associated with the ER lumen) DGAT activity. We tried using two different DG species as acceptor substrates for DGAT, dipalmitoylglycerol and dioleoylglycerol (with the corresponding acyl-CoAs as donors), but the former failed to yield reproducible and reliable results for the latent component of DGAT activity (data not shown). This may either indicate true substrate preference or be due to differences in the efficacy of substrate delivery to the luminal ER space, attributable to the biophysical characteristics of the substrates.

The total, overt, and latent DGAT activities assessed using dioleoylglycerol as an acceptor and [^{3}H]oleoyl-CoA as a donor were found to be similar in the HepG2-EV and HepG2-SMS1 cell lines (Fig. 5, *D* and *E*). This implies that SMS1 overexpression does not affect the active DGAT enzyme levels. Treatment of HepG2-EV cells with 1 mM palmitic acid led to a 2-fold increase in the latent but not overt DGAT activity. This probably reflects palmitate-related increases in the endogenous DGs that are being acylated with the exogenously added radioactive Acyl-CoA. However, the effect is not seen in HepG2-SMS1 cells (Fig. 5*F*). This is consistent with the differences in the rates of TG synthesis seen between HepG2-EV and HepG2-SMS1 cells when BODIPY- or [^{3}H]palmitate was used (Figs. 4*B* and 5*A*).

The levels of TG in the cell culture medium of HepG2-EV and HepG2-SMS1 were also similar (Fig. 5*B*). Finally, analyses of the oxygen consumption rates in intact cells also did not reveal any differences between the two cell lines (Fig. 5*C*). Together, these results ruled out the possibility that SMS1 overexpression interferes with the basal activity of DGAT, TG secretion, or with the overall mitochondrial functions.

Evidence for Increased Fatty Acid Remodeling of TG in the HepG2-SMS1 Cells—The fatty acid composition of TG in the two lines was compared using a lipidomic approach (Table 1). An S-plot obtained from orthogonal partial least squares-discriminant analysis (OPLS-DA) of the data derived from cells under basal conditions (Fig. 6*A*) and after palmitate stimulation (Fig. 6*B*), showed that the abundance of TG containing polyunsaturated fatty acids (*i.e.* 18:1/20:3/22:6, 18:3/18:3/22:4, 18:3/20:3/22:5, 16:0/18:2/18:3, 16:0/18:1/20:4, and 16:0/18:1/22:5) was between 2 and 4 times higher in the HepG2-SMS1 cells compared with the HepG2-EV cells. Typically, polyunsaturated fatty acids are not added to the glycerol backbone during the *de novo* glycerophosphate synthesis but rather as a result of deacylation/reacylation of either glycerophospholipids or TG. One possible reason for elevated deacylation/reacylation of TG could be a limited supply with DG precursor for the DGAT pathway. Alternatively, studies in yeast and mammals have indicated a possible connection between the TG deacylation/reacylation and the *de novo* synthesis of glycerophospholipids, suggesting that increased esterification of polyunsaturated fatty acids into TG may be the purpose of enhanced *de novo* glycerolipid synthesis (14, 15).

Increased de Novo Synthesis of Phosphatidylcholine in HepG2-SMS1 Cells—To directly assess the effects SMS1 has on glycerophospholipid synthesis, we followed the incorporation of radioactive palmitic acid in all major lipid classes. The advantage of using this label (instead of glycerol or acetate) was 2-fold. First, it allowed for simultaneously labeling TG, glycerophospholipids, and sphingolipids. Second, it was more practical as a tracer for the studies involving high and low palmitate concentrations. Cells were cultured in the presence of 0.1 or 1 mM non-labeled palmitic acid, mixed with the radioactive [^{3}H]palmitate (final specific labeling of 50 μCi/mmol). Incorporation of the label into each lipid class was quantified after TLC separation and elution of the lipids from the silica. As shown earlier, the SMS1-overexpressing cells incorporate [^{3}H]palmitate into SM more readily than their control counterparts. The influx of label into SM is further increased upon treatment with 1 mM palmitic acid (Fig. 7*A*). Labeling of TG was also readily seen and increased almost 15-fold in the presence of 1 mM palmitate (Fig. 7*B*). Notably, as seen with the mass measurements and Oil Red-O staining, this effect is significantly reduced (by almost 50%) in the SMS1-overexpressing cells, confirming that SMS1 overexpression suppresses the flux through the TG pathway.

The treatment with 1 mM palmitic acid also led to increased flux through the synthetic pathways of all glycerolipids that we

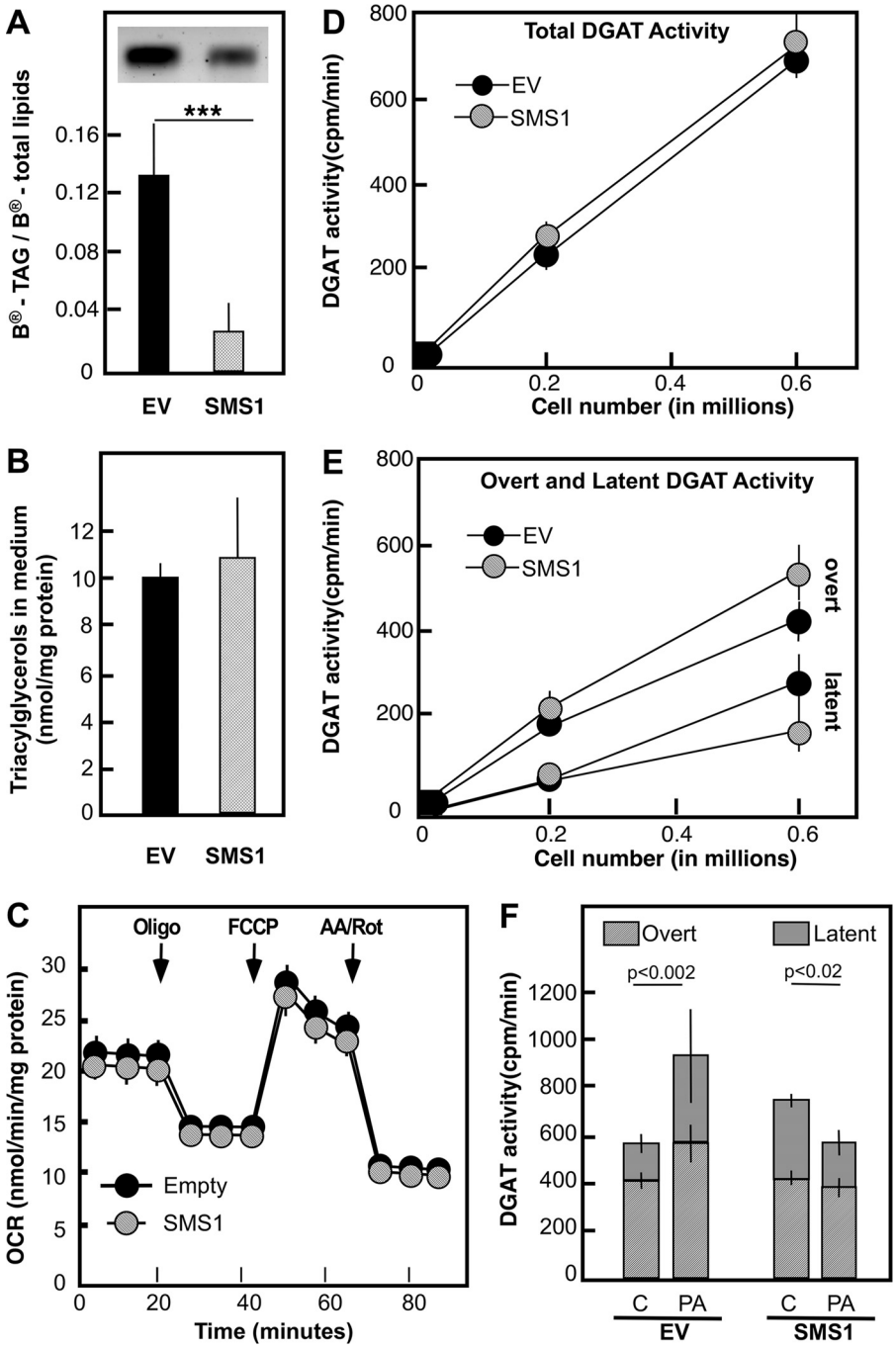

FIGURE 5. **Effects of SMS1 overexpression on DGAT activity, TG secretion, and mitochondrial bioenergetics.** HepG2 cells stably overexpressing the human SMS1 or EV controls. *A*, *de novo* TG biosynthesis assessed using BODIPY®-labeled palmitic acid as a tracer (8 μM for 18 h). Levels of BODIPY®-TG were quantified after TLC separation by scanning the plates using a Typhoon imager and normalizing the intensity of the TG bands to the intensity of the total lipid extract. *B*, TG levels in conditioned medium (18 h) were measured following extraction with Dole's reagent and separation on a TLC plate. *C*, OCRs of HepG2-SMS1 and HepG2-EV cells. A mitochondrial respiration assay was done using an XF96 extracellular flux analyzer (Seahorse Biosciences). The culture medium was serum-free and contained 10 mM glucose, 3 mM glutamine, and 1 mM pyruvate. Inhibitors (1.25 μM oligomycin, 1.0 μM FCCP, and 2.0 μM antimycin A or 2.0 μM rotenone) were injected at the indicated time points to block different components of the electron transport chain. *D* and *E*, DGAT activity (total (*D*) and overt and latent (*E*)) measured in permeabilized cells as described under "Experimental Procedures." Latent activity was calculated as the difference between total and overt activities. Mean values ± S.D. (*error bars*) are shown ($n = 3$ dishes/point). *F*, effect of palmitic acid on DGAT activity. HepG2-EV or HepG2-SMS1 cells were cultured for 18 h in the presence of either 0.5 mM BSA as a vehicle control or 1 mM palmitic acid delivered as a BSA complex (2:1, mol/mol). Overt and latent DGAT activity was measured as described under "Experimental Procedures." Results were confirmed in at least two independent experiments, and representative data are shown. ***, $p < 0.001$ (*A*) or as indicated (*F*) according to Student's *t* test. $n = 3$ dishes/point. Results were confirmed in at least two independent experiments.

measured (PC, PE, phosphatidylserine (PS), phosphatidic acid, and DG) with a magnitude ranging from 2- to 3-fold (Fig. 7, *C–G*). However, with the notable exception of PC, none of the glycerophospholipids were affected by SMS1 overexpression (Fig. 7, *C–F*). For PC, the rate of [^{3}H]palmitate incorporation was substantially higher in the HepG2-SMS1 cells, both at low

TABLE 1

Effect of SMS1 overexpression on TAG fatty acid composition in control conditions and in the presence of 1 mM palmitic acid

The identification of each TG lipid species is based on exact monoisotopic precursor mass, fragment ion information, and theoretical isotopic distribution.

			1 mM palmitic acid, HepG2-SMS1 *versus* HepG2-EV		Vehicle, HepG2-SMS1 *versus* HepG2-EV	
m/z[a]	Accepted identification[b]	Total carbon: double bond	-Fold change	p(corr)	-Fold change	p(corr)
970.7855	TG (18:3/20:3/22:5)	TG (60:11)	11.1	0.997344	3.8	0.968865
972.8017	TG (18:1/20:3/22:6)	TG (60:10)	7.2	0.995491	2.5	0.973176
944.7698	TG (18:3/18:3/22:4)	TG (58:10)	6.2	0.996561	2.4	0.963495
948.8008	TG (18:1/18:4/22:3)	TG (58:8)	4.5	0.994698	1.6	0.941047
924.8014	TG (16:0/18:1/22:5)	TG (56:6)	4.2	0.997911	2.1	0.957018
898.7848	TG (16:0/18:1/20:4)	TG (54:5)	3.8	0.997447	2.1	0.955878
894.7545	TG (16:0/18:3:20:4)	TG (54:7)	ND[c]	ND	1.7	0.957635
926.8156	TG (16:0/18:1/18:2)	TG (52:3)	2.9	0.989006	1.5	0.919795
950.8175	TG (18:3/20:1/20:3)	TG (58:7)	2.7	0.986254	1.7	0.944278
948.8008	TG (18:1/18:4/22:3)	TG (58:8)	ND	ND	1.7	0.941047
922.7857	TG (16:0/18:1/22:6)	TG (56:7)	2.6	0.985647	1.4	0.917071
952.8328	TG (18:0/18:2/22:4)	TG (58:6)	2.6	0.992549	1.6	0.931402
874.7859	TG (16:1/18:0/22:4)	TG (56:5)	2.3	0.995110	ND	ND
902.8155	TG (16:0/18:0/20:3)	TG (54:3)	2.2	0.973230	1.1	0.801826
926.8173	TG (16:0/20:1/20:4)	TG (56:5)	2.1	0.983169	2.0	0.919795
870.7542	TG (16:0/18:2/18:3)	TG (52:5)	2.0	0.989413	1.8	0.949937
896.7698	TG (16:0/16:1/22:5)	TG (54:6)	2.0	0.954632	1.4	0.878744
896.7707	TG (16:0/18:1/20:5)	TG (54:6)	2.0	0.982693	1.7	0.96172
876.7998	TG (16:0/18:0/18:2)	TG (54:2)	1.8	0.940230	1.2	0.804526
872.7705	TG (16:0/16:0/20:4)	TG (52:4)	1.7	0.973257	1.2	0.871994
824.7703	TG (16:0/16:0/16:0)	TG (48:0)	1.2	0.831157	ND	ND
850.7859	TG (16:0/16:0/18:1)	TG (50:1)	0.90	−0.648602	1.4	0.883765
822.7545	TG (16:0/16:0/16:1)	TG (48:1)	0.53	−0.970125	1.2	0.824069
794.7232	TG (14:0/16:0/16:1)	TG (46:1)	0.48	−0.984013	ND	ND
848.7702	TG (16:0/16:0/18:2)	TG (50:2)	0.42	−0.920163	ND	ND
820.7388	TG (16:0/16:1/16:1)	TG (48:2)	0.27	−0.954241	ND	ND

[a] All TG were identified as ammonium adducts.
[b] *sn*-1, *sn*-2, and *sn*-3 fatty acid assignments are arbitrary.
[c] ND, not detected.

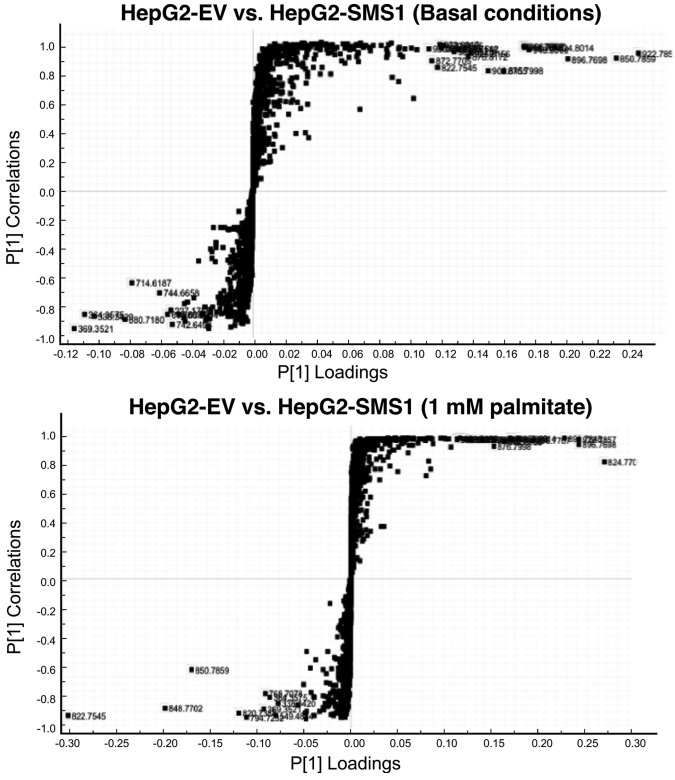

FIGURE 6. **TG species distribution in SMS1 and control cells.** HepG2 cells were cultured for 18 h in the presence of either 0.5 mM BSA as a vehicle control (*upper panel*) or 1 mM palmitic acid delivered as a BSA complex (2:1, mol/mol) (*lower panel*) for 18 h. TG fatty acid composition measured by mass spectrometry as described under "Experimental Procedures." The graphs represent S-plots of OPLS-DA of TG fatty acid composition and indicate the major features that contributed to the group difference between HepG2-EV and HepG2-SMS1 in each case. Data are the average of three replicates.

and high palmitate concentrations (Fig. 7*C*). Mass measurements confirmed that SMS1 cells have higher PC content (40% more), whereas the levels of PE and PS are similar to those in HepG2-EV controls (data not shown).

Together, these results show that whereas the elevated supply of exogenous palmitic acid leads to its increased incorporation into all lipids, the activity of SMS1 seemingly affects the way that palmitate is partitioned among the different lipid classes, favoring PC and SM at the expense of TG.

HepG2-SMS1 Cells Have an Enhanced Rate of PC Synthesis—The observation that the PC mass and labeling were higher in HepG2-SMS1 cells was unexpected because PC is a substrate in the reaction catalyzed by SMS1. To independently study the rate of PC synthesis and its conversion to SM, [^{14}C]choline was used. Incorporation of [^{14}C]choline into PC and SM increased gradually over time but was substantially lower for SM in both SMS1-overexpressing and control cells (Fig. 8). This is consistent with the role of PC as a donor of [^{14}C]choline for SM. As expected, the HepG2-SMS1 cells had higher label incorporation into SM as compared with the control HepG2-EV cells (Fig. 8*B*). However, the SMS1-overexpressing cells also exhibited elevated PC labeling (by 24 pCi/mg protein at 30 min and by 30 pCi/mg protein at 1 h) than the control cells (Fig. 8*A*). These results suggest that increased synthesis of SM in HepG2-SMS1 cells probably leads to a compensatory activation of *de novo* synthesis of PC, probably in the ER.

Discussion

The family of sphingomyelin synthases possesses the unique ability to control the levels of two bioactive lipid metabolites, DG and ceramide (16–19). This fact has instigated several stud-

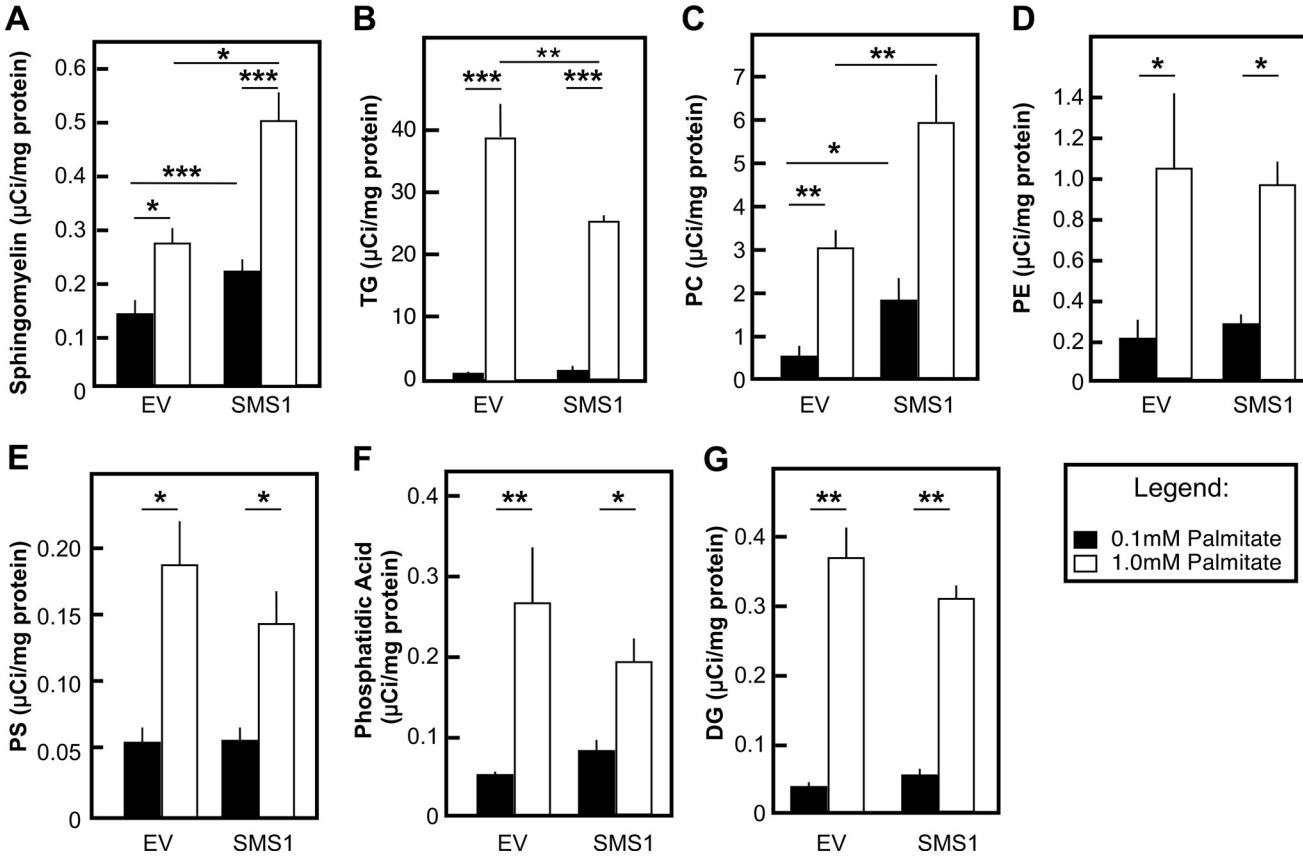

FIGURE 7. **Effects of SMS1 overexpression and palmitic acid on the synthesis of major lipid classes.** HepG2-SMS1 and EV control cells were supplemented with [^{3}H]palmitic acid at low (0.1 mM) or high (1.0 mM) concentration for 18 h. The specific labeling in each case was kept at 50 mCi/mmol. Lipids were extracted and separated by TLC as described under "Experimental Procedures." Radioactivity from the individual bands was quantified by scintillation counting. *A*, SM; *B*, TG; *C*, phosphatidylcholine; *D*, phosphatidylethanolamine; *E*, phosphatidylserine; *F*, phosphatidic acid; *G*, DG. According to two-way analysis of variance, a strong statistically significant main effect of palmitate treatment was detected for all lipids. The main effects of SMS1 overexpression on TG, PC, and DG were also statistically significant. A statistically significant interaction effect was seen for SM and TG. Results of Bonferroni post-test analyses are shown (*, $p < 0.05$; **, $p < 0.01$; ***, $p < 0.001$). Results were confirmed in two independent experiments. *Error bars*, S.D.

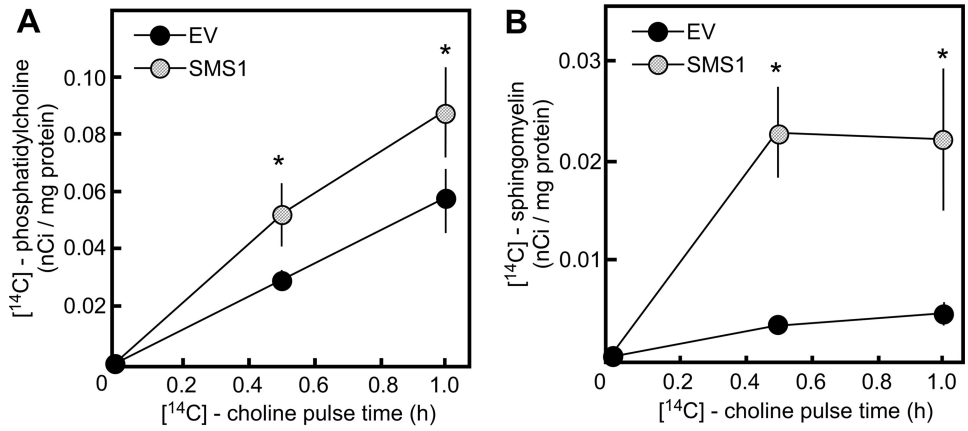

FIGURE 8. **Effect of SMS1 overexpression on the *de novo* synthesis of PC.** HepG2-SMS1 and EV control cells were cultured in complete growth medium supplemented with 0.3 μCi/well radiolabeled [^{14}C]choline chloride for the indicated periods of time. Lipids were extracted and separated by TLC as described under "Experimental Procedures." Radioactivity from the corresponding bands was quantified by scintillation counting. *A*, phosphatidylcholine; *B*, sphingomyelin. Data shown are the average ± S.D. (*error bars*), $n = 3$ (*, $p < 0.05$). Results were confirmed in two independent experiments.

ies utilizing transient overexpression to investigate the fate of SMS-derived DG and the resulting functional implications. SMS1, which is localized in the Golgi and is responsible for the synthesis of the bulk of cellular SM, has been a particular focus. These studies found that cellular homeostasis of DG is indeed affected by the rate of SM synthesis, but the exact effects vary depending on cell type. In some cases, SMS1-derived DG triggered localized cellular responses, like PKD translocation to the Golgi (20), whereas in other cells, DG was found to rapidly reincorporate back into PC (21). The data presented here show that in hepatocytes, the increased flux through the SMS1 pathway has a profound effect on the overall lipid homeostasis,

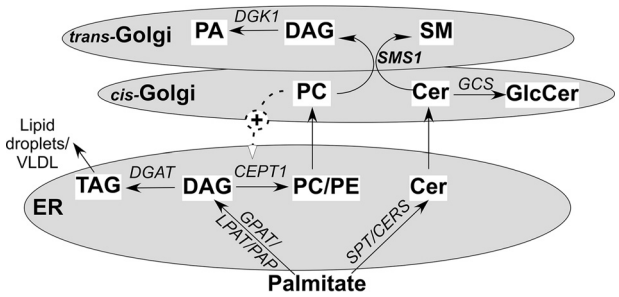

FIGURE 9. **Proposed mechanism for the SMS1 regulation of TG synthesis.** The figure illustrates the main pathways for glycerolipid and sphingolipid synthesis and their respective localization in the ER and Golgi apparatus. Chronic increases in SMS1 in the *trans*-Golgi generate a signal of enhanced utilization of PC, resulting in the stimulation of PC synthesis in the ER via CEPT1. As a result, the pool of DG substrate available for TG synthesis is diminished, causing a decline in TG synthesis. A change in the fatty acid composition of available DG substrate might also influence its metabolic conversion toward PC rather than TG synthesis due to different substrate preferences of CEPT1 and DGAT1 (see "Discussion"). Also shown are the two routes for utilization of palmitic acid in sphingolipid and glycerolipid synthesis. *CERS*, ceramide synthase; *DGK1*, diacylglycerol kinase 1; *GlcCer*, glucosylceramide; *GPAT*, glycero-3-phosphate acyltransferase; *LPAT*, lysophosphatidic acid acyltransferase; *PA*, phosphatidic acid; *PAP*, phosphatidic acid phosphatase.

including that of glycosphingolipids, glycerophospholipids, and TG. The major observation reported here is that SMS1 activity seemingly affects the partitioning of DG molecules into the TG and glycerophospholipid synthetic pathways (Fig. 9). Because SMS1 is localized in the *trans*-Golgi apparatus, whereas the synthesis of DG for TG and PC/PE synthesis happens in the ER, the SMS1 activity most likely affects DG partitioning indirectly. The exact molecular mechanisms behind the SMS1 effects are currently unknown. Several components have, however, emerged. For one, PC is essential for membrane biogenesis and cell survival; therefore, all mammalian cells have mechanisms in place to detect even the smallest declines in PC levels (22). Once engaged, these mechanisms lead to rapid activation of the *de novo* PC synthesis. The known stimuli for initiating these mechanisms involve products of PC degradation via phospholipase D (*i.e.* phosphatidic acid), phospholipase A2 (*i.e.* arachidonic acid), or the putative PC-specific phospholipase C (*i.e.* DG). Our studies suggest that chronic up-regulation of SMS1 activity can also cause activation of PC *de novo* synthesis as a consequence of the increased consumption of PC in the Golgi. Indicatively, one earlier study on SMS suggested that SMS activity could account for many of the functions that have been proposed for the PC-specific phospholipase C, given the similar properties of the two enzymes (18). Second, the fatty acid composition of the DG substrate is known to influence the pathway for the metabolic conversion of DG. Dipalmitoylglycerol, for example, is a poor substrate for DGAT1, one of the two DGATs known to synthesize TG (23), but is readily utilized by CEPT1 (24). Also in this study, although we did not analyze the fatty acid composition of PC or PE, a shift was seen in the fatty acid composition of TG (toward more unsaturated fatty acids and less palmitate). In addition, one cannot completely exclude the possibility that SMS1 may affect DGAT activity. In hepatocytes, total DGAT is the sum of two distinct, biochemically defined pools of activity: the overt or cytosolic activity and the latent activity localized in the ER lumen (25, 26). Palmitate treatment seems to increase the latent component in control cells but not in HepG2-SMS1 cells. This difference between the two cell lines may simply reflect the shift in the substrate utilization pathway described above, resulting in fewer endogenous substrates available for the reaction in HepG2-SMS1 cells; however, it is also possible that SMS1 induces changes in the interacting partners of the DGAT enzymes and/or engenders selective posttranslational modifications affecting active site exposure to the ER lumen. At present, the enzyme accountable for the latent DGAT activity is not clearly defined (27). Two non-homologous proteins, DGAT1 and DGAT2, both of which are integral ER proteins, contribute to total hepatic DGAT. Some studies seem to suggest that DGAT1 may contribute to both the latent and the overt activity, whereas the topology of DGAT2 suggests that it contributes only to the overt activity (28). Because DGAT1 is also the enzyme with a preference for unsaturated fatty acids, it seems reasonable to investigate the potential link between DGAT1 and SMS1 in follow-up studies.

We should point out that the concept of coordinated and inverse regulation of glycerophospholipid and TG synthesis, via competition for the available DG pool, is based on previous studies done by others. A cornerstone of this concept is the notion that the rate of phospholipid/TG synthesis is determined by the amount of DG substrate available from the enzymatic activities upstream of the DGAT and the CEPT1 and/or selective substrate specificity of the enzymes (29). It has been shown, for example, that enforced expression of CTP:phosphocholine cytidylyltransferase 1 (CCT1), which is the first rate-limiting step in *de novo* PC synthesis and provides the CDP-choline substrate for CEPT1, stimulates PC biosynthesis while reducing that of TG (8). In contrast, inhibition of CCT activity diverts newly synthesized DG toward the TG synthetic pathway and leads to TG accumulation (8). Similar correlations are seen *in vivo*, because liver-specific deletion of CCT1 is associated with the development of mild steatosis (31). Deletion of the phosphoethanolamine cytidylyltransferase, which catalyzes the rate-limiting step for PE synthesis and provides the CDP-ethanolamine substrate for CEPT1, has similarly been shown to result in hepatic steatosis (8). Modulating the flux through the TG pathways also can affect the rate of phospholipid synthesis, and overexpression of DGAT1 was found to inhibit the synthesis of glycerophospholipids (10), confirming that the DG pool in the ER is shared between TG and glycerophospholipid synthesis.

Another interesting metabolic interaction seen in our studies is between SMS1 and Hex-Cer synthesis. The synthesis of Hex-Cer occurs either in the Golgi (where the GCS is localized) or in the ER (where the non-essential galactosylceramide synthase resides). Our experiments seem to indicate that the overexpressed SMS1 acts on a pool of ceramide designated for GCS. This is evidenced by the decline seen in the levels of Hex-Cer in SMS1-overexpressing cells (based on mass spectrometry analysis and *in situ* labeling with NBD-ceramide, which is a Golgi-targeted ceramide analog (32)). These observations are consistent with earlier studies with PDMP (a GCS inhibitor) that reported significant increases in SM levels in PDMP-treated cells (33, 34). Also, recent studies with SMS1 knock-out mice have shown them to have elevated glucosylceramide synthesis (35).

It is likely, however, that there are pools of ceramide available only to GCS and not to SMS1. Unlike SM synthesis (which occurs at the luminal surface of the *trans*-Golgi apparatus), GCS appears to be more widely distributed, with substantial amounts of synthesis detected also in the cytosolic face of the heavy (*cis*/*medial*) Golgi apparatus subfraction (36). Also, the pathways of ER-to-Golgi transport of ceramide utilized for SMS1 and GCS are apparently different, with ceramide transfer protein, CerT1, providing ceramide exclusively for SMS1 (37). Finally, PDMP treatment also results in accumulation of ceramide, indicating that not all of the GCS-utilized ceramides were immediately available to SMS1 (33) (data not shown).

Several seminal studies have shown that diets rich in saturated fats stimulate the *de novo* ceramide synthesis in liver, muscle, fat, and some other tissues (38). The consequent increases in ceramide and glucosylceramide have been implicated in the onset of insulin resistance, via either direct inhibitory effects on the PI3K pathways engaged by the insulin receptor (via ceramide) (39) or by interference with the lipid rafts (via glucosylceramide) (40). The direct effects of palmitate on sphingolipid metabolism, however, are far less clear. Our results are consistent with observations made by others that palmitate alone does indeed stimulate *de novo* ceramide synthesis. However, we also find that the increases seen in C16-ceramide surpass in magnitude those for other ceramide species. This observation is in agreement with similar findings in endothelial cells (41). It should be noted that we saw little palmitate-associated toxicity in our system. This is in contrast to other studies, done in the same cell line, which report that as much as 30% of the cells undergo apoptosis in response to palmitic acid added at concentrations as low as 0.75 mM (42, 43). One possible reason for this discrepancy is differences in the method by which the palmitate was delivered. In our studies, the fatty acid was delivered as a complex with delipidated BSA at a molar ratio of 2:1, which guaranteed that all palmitate was bound to BSA. In comparison, Martínez *et al.* (42) used a palmitate/BSA ratio ranging from 3:1 to 6:1, whereas Rojas *et al.* (43) used a molar ratio of 7:1 to reflect the correlations seen *in vivo* between adverse effects and elevated free, non-albumin-bound fatty acid content (42). Other studies that have also reported palmitate-associated toxicity have used DMSO as a delivery vehicle. DMSO is nonphysiological; hence, this delivery method is not comparable with the BSA-mediated delivery. In conclusion, the findings presented here contribute to better understanding of the biochemical properties of SMS1 and reveal a novel metabolic interaction between the sphingolipid and the glycerolipid synthetic pathways.

Experimental Procedures

Materials

N-Hexanoyl-((*N*-(7-nitrobenz-2-oxa-1,3-diazol-4-yl) amino)-sphingosine, *N*-hexanoyl-sphingosine-1 phosphocholine, and BODIPY® FL C16 (4,4-difluoro-5,7-dimethyl-4-bora-3a,4a-diaza-*s*-indacene-3-hexadecanoic acid) were purchased from Life Technologies, Inc. Bovine brain sphingomyelin, egg phosphatidylcholine, phosphatidylethanolamine, phosphatidylserine, and 1,2-dioleoyl-*sn*-glycerol were purchased from Avanti Polar Lipids (Alabaster, AL). Geneticin (G418) sulfate and alamethicin were from Santa Cruz Biotechnology, Inc. (Dallas, TX). Essentially fatty acid-free BSA, triolein, oleoyl-coenzyme A lithium salt, Oil Red-O, and digitonin were purchased from Sigma-Aldrich. TLC plates were from Waters Corp. (Milford, MA). The total protein determination kit (DC Protein Assay) was from Bio-Rad. All other reagents were from Fisher.

Cloning of Full-length Human V5-tagged Sgms1

PCR-amplified sequence encoding the full-length human SMS1 was cloned into pcDNA3.1/V5-His-TOPO vector containing neomycin selection marker (Invitrogen). The resulting SMS1-pcDNA3.1/V5-His-TOPO plasmid was used to transfect HepG2 cells.

Cell Culture, Transfections, and Treatments

HepG2 cells obtained from ATTC (Manassas, VA) were maintained in MEM (Invitrogen) supplemented with 10% FBS and 1% penicillin/streptomycin in a humidified atmosphere of 95% air and 5% CO_2 at 37 °C. For transient transfection experiments, cells were grown to subconfluence in 6-well plates and transfected with 2 μg/well of SMS1-pcDNA3.1/V5-His-TOPO or empty vector (EV) control, using Trans IT 2020 (Mirus Bio LLC, Madison, WI) following the manufacturer's instructions. For stable transfection, HepG2 cells were initially transfected using FuGENE® HD transfection reagent (Promega, Madison, WI), and stable clones were selected in growth medium containing 2 mg/ml Geneticin (G418) under continuous pressure for 3 weeks. Single cell colonies were established and expanded in the presence of G418. The single cell colony with appropriate subcellular localization and highest expression of SMS1 protein, as judged by indirect immunofluorescence, was chosen for future experiments and referred to as HepG2-SMS1 cells. Cells stably transfected with the empty vector (HepG2-EV) were used as control.

To stimulate *de novo* synthesis of ceramide, HepG2-SMS1 and HepG2-EV control cells maintained in growth-selective MEM (2 mg/ml G418) were grown to subconfluence in 6-well plates and treated for 18 h with BSA vehicle or with 1 mM palmitic acid delivered as a complex with BSA (2:1, mol/mol). For these treatments, the L-serine concentration of MEM was increased from 0.1 to 0.5 mM to ensure that serine levels are not limiting in the SPT reaction.

Indirect Immunofluorescence

Cells were grown on coverslips to subconfluence and fixed with 3.7% paraformaldehyde in PBS. After quenching the autofluorescence with 50 mM NH_4Cl in PBS, the cells were permeabilized with 0.2% Triton X-100 and then incubated with blocking buffer (0.5% BSA in PBS) for 1 h at room temperature. Incubation of the cells with mouse monoclonal anti-V5 antibody (Invitrogen) was performed overnight at 4 °C, followed by incubation with anti mouse FITC-conjugated secondary antibody (1 h at room temperature). Cells were counterstained with 1 μg/ml rhodamine-labeled wheat germ agglutinin (VectorLabs, Burlingame, CA) to visualize Golgi. Mounting

on slides was performed in DAPI-Vectashield mounting medium (VectorLabs).

Labeling Experiments

HepG2-SMS1 and HepG2-EV cells maintained in growth-selective MEM (2 mg/ml G418) were grown to subconfluence in 6-well plates and labeled with various lipid precursors. *In situ* labeling with NBD-Cer at a final concentration of 4 μM was done as described previously (17). PDMP (25 μM), the inhibitor of GCS, was added to the cell culture medium 1 h before the fluorescent ceramide. The levels of NBD-ceramide and its metabolic products were measured using a high performance liquid chromatograph equipped with a fluorescence detector. *In situ* labeling with BODIPY® FL C16 was done in serum-deficient medium containing 0.5 mM fatty acid-free BSA at a final concentration of 8 μM for 18 h. The BODIPY-labeled lipids were separated as described below and analyzed using a Typhoon imaging system. Labeling with [^{3}H]palmitic acid ([9,10-^{3}H]palmitic acid; 30–60 Ci/mmol, American Radiochemical Corp., St. Louis, MO) was done for 18 h. The [^{3}H]palmitic acid was mixed with cold palmitate and delivered to the cells as a complex with BSA (2:1, mol/mol) at low (0.1 mM) or high (1 mM) concentrations, while maintaining the same specific labeling (50 μCi/mmol). Cells were also labeled with [^{14}C]choline chloride ([*methyl*-^{14}C]choline chloride, 50–60 mCi/mmol; American Radiochemical Corp.) (0.3 μCi/well) in complete growth medium for different periods of time. Following treatment, cells were harvested, and lipids were extracted in the presence of cold carriers and analyzed as described below. Radioactivity from individual bands was quantified by scintillation counting after scraping the silica off of the plate.

Lipid Extraction and Analyses

Phospholipids—Lipids were extracted from cells by the method of Bligh and Dyer, modified as described previously (44), and analyzed by thin layer chromatography on silica gel 60 plates (10 × 20 cm) using chloroform, methanol, triethylamine, 2-propanol, 0.25% potassium chloride (30:9:18:25:6, v/v/v/v/v) as the developing solvent. The regions corresponding to SM, PC, PS, and PE were sprayed with 50% sulfuric acid and incubated at 190–200 °C for 3.5 h. Inorganic phosphorus was quantified according to the method of Kahovcová and Odavić (45).

Tri- and Diacylglycerols—Lipid extracts from cells were prepared using chloroform/methanol (2:1, v/v). Extracts from the cell culture medium were prepared using Dole's reagent (isopropyl alcohol, *n*-heptane, 1 N sulfuric acid (40:10:1, v/v/v)). To isolate DG and TG, the total lipid extracts were subjected to thin layer chromatography on silica gel 60 plates (10 × 20 cm), using chloroform/acetone/acetic acid (95.5:4:0.5, v/v/v) as the developing solvent (46). The regions migrating with the trioleoyl and dioleoyl standards (Avanti Polar Lipids, Inc., Alabaster, AL) were scraped off of the plates, and lipids were eluted from the silica using 2 ml of chloroform/methanol/water/acetic acid (100:100:5:0.5, v/v/v/v). Elutes were dried under vacuum, the lipids were dissolved in isopropyl alcohol, and the masses of TG and DG were quantified using the Triglyceride-M kit (Wako, Japan) following the manufacturer's instructions.

Cholesterol—Total cholesterol (free and esterified) in whole cell lipid extracts prepared as described for TG was determined according to the method of Sperry and Webb (47).

Mass Spectrometry Analysis of Sphingomyelin, Ceramide, and Hexosylceramide

The sphingolipid analysis was conducted by electrospray ionization tandem mass spectrometry using an ABI 4000 quadrupole-linear ion trap mass spectrometer (48) with internal standards from Avanti Polar Lipids (Alabaster, AL).

Ultrahigh Performance Supercritical Fluid Chromatography and Mass Spectrometry Analysis of TG

Supercritical fluid chromatography experiments were performed using a Waters Acquity UPC2 system (Milford, MA). Experiments were carried out using an ACQUITY UPC2 HSS C18 SB column (150 × 3.0 mm, 1.8 μm) at a temperature of 25 °C. Mobile phase A consisted of compressed CO_2, and mobile phase B consisted of 100% acetonitrile. The flow rate was maintained at 1.2 ml/min with an injection volume of 0.5 μl. Backpressure was maintained at 1500 p.s.i. The elution gradient was 10–40% mobile phase B in 10 min and hold at the initial condition of 10% B for 1 min.

Mass spectrometry was performed using Xevo G2-S QTof (Waters Corp., Milford, MA). The solvent flow was split using a pre-back pressure regulator flow Upchurch cross 1/16 PEEK splitter. CO_2-miscible make-up solvent (0.5% NH_4OH in methanol), delivered by an HPLC 515 make-up pump (Waters Corp.), was added at a flow rate of 0.2 ml/min and mixed with the chromatographic effluent to aid ionization. A fraction of the total flow was directed to the electrospray ionization source through a transfer line, whereas the remaining mobile phase was directed to the back pressure regulator PEEK connection. The electrospray ionization source was operated in positive ionization mode with capillary and cone voltages of +3 kV and 30 V, respectively. The source temperature, cone gas flow, desolvation temperature, and desolvation gas flow were set at 150 °C, 10 liters/h, 500 °C, and 600 liters/h, respectively. Data were acquired in the range of 100–1200 *m/z*. Data handling and instrument control were performed with Masslynx version 4.1 (Waters Corp.). Multivariate data analysis and TG identification were performed using Progenesis QI version 2.0 (Nonlinear Dynamics, Newcastle, UK). Results were shown using the S-plot for OPLS-DA.

DGAT Activity Assay

Measurement of overt and latent DGAT activity was performed in permeabilized cells as described previously (49). Briefly, for overt activity, cells were trypsinized, washed, and permeabilized by incubating on ice for 30 min in artificial "cytoskeleton" medium containing 30 μg/ml digitonin. Aliquots were taken and subsequently incubated with alamethicin (20 μg/ml) for 30 min on ice to expose the remaining DGAT activity found on the luminal side of the ER (known as latent). After removing all detergents, cells were placed in Tris-HCl reaction buffer (pH 7.4) containing 10 mM $MgCl_2$ and 250 mM sucrose, 500 μM 1,2-dioleoylglycerol or 1,2-dipalmitoylglycerol, BSA (2.5 mg/ml), and 0.6% DMSO. The mixtures were incubated at

37 °C for 5 min in a heating block. The reaction was then initiated by the addition of oleoyl-[1-^{14}C]CoA or palmitoyl-[1-^{14}C]CoA (American Radiochemical Corp.) (50 μM, specific activity of 1 mCi/mmol). Following a 5-min incubation, the reaction was stopped by the addition of 1.5 ml of isopropyl alcohol/*n*-heptane/water (80:20:2, v/v/v). After a 5-min incubation at room temperature, 1 ml of heptane and 0.5 ml of water were added, and the tubes were vortexed. Phases were allowed to separate, and the organic layer was removed and washed twice with 2 ml of 0.5 N sodium hydroxide/ethanol/water (10:50:50, v/v/v) (30). Aliquots from the final organic layer were taken and mixed with scintillation fluid, and radioactivity was quantified using a scintillation counter.

Oil Red-O Staining of Cultured Cells

Cells grown on coverslips were washed three times with PBS and fixed for 30 min at room temperature in freshly prepared 3.7% formaldehyde solution in PBS. After several washes, cells were incubated for 20 min with 0.2% Oil Red-O in 60% isopropyl alcohol, followed by brief contrastaining with hematoxylin. Coverslips were then mounted using Aqua-Mount® mounting medium (Lerner Laboratories, Pittsburgh, PA).

Mitochondrial Respiration Assay

Mitochondrial function was analyzed using the Seahorse XF Cell Mito Stress Test Kit and XF96 extracellular flux analyzer (Seahorse Bioscience), following the manufacturer's instructions. Briefly, cells were seeded in 96-well plates, and assays were performed 2 days latter in serum-free culture medium containing 10 mM glucose, 3 mM glutamine, and 1 mM pyruvate. Inhibitors of the electron transport chain proteins (1.25 μM oligomycin, 1.0 μM FCCP, and 2.0 μM antimycin A or 2.0 μM rotenone) were injected at the indicated time points. Measurements of oxygen consumption rate (OCR) were taken at the indicated times (n = 6–8). Analyses were performed with Wave software and XF Report Generators (Seahorse Bioscience).

Author Contributions—G. M. D. established cell lines, performed most of the experiments, and prepared figures and parts of the manuscript. P. P. D. cloned SMS1 and prepared plasmid for transfections. G. I. and M. W. performed the analyses of TG by mass spectrometry; S. B. K. completed the mass spectrometric analyses of sphingolipids; A. A. K. participated in manuscript editing and DGAT analyses; A. H. M. participated in analysis of sphingolipids and critically evaluated the manuscript; and M. N. N.-K. participated in experimental design, data interpretation, and manuscript preparation. All authors approved the final version of the manuscript.

Acknowledgments—We thank Dr. J. Holthuis (Utrecht University) for providing the SMS1 construct that was used as a reference and Dr. M. Mitov (University of Kentucky) for measuring the OCR in the Redox Metabolism Shared Resource Facility of the University of Kentucky Markey Cancer Center (supported by NCI, National Institutes of Health, Grant P30CA177558).

References

1. Tafesse, F. G., Huitema, K., Hermansson, M., van der Poel, S., van den Dikkenberg, J., Uphoff, A., Somerharju, P., and Holthuis, J. C. (2007) Both sphingomyelin synthases SMS1 and SMS2 are required for sphingomyelin homeostasis and growth in human HeLa cells. *J. Biol. Chem.* **282,** 17537–17547
2. Futerman, A. H., Stieger, B., Hubbard, A. L., and Pagano, R. E. (1990) Sphingomyelin synthesis in rat liver occurs predominantly at the *cis* and *medial* cisternae of the Golgi apparatus. *J. Biol. Chem.* **265,** 8650–8657
3. Merrill, A. H., Jr., and Wang, E. (1986) Biosynthesis of long-chain (sphingoid) bases from serine by LM cells: evidence for introduction of the 4-*trans*-double bond after *de novo* biosynthesis of *N*-acylsphinganine(s). *J. Biol. Chem.* **261,** 3764–3769
4. Hanada, K. (2010) Intracellular trafficking of ceramide by ceramide transfer protein. *Proc. Jpn. Acad. Ser. B Phys. Biol. Sci.* **86,** 426–437
5. Kennedy, E. P. (1957) Metabolism of lipides. *Annu. Rev. Biochem.* **26,** 119–148
6. Declercq, P. E., Haagsman, H. P., Van Veldhoven, P., Debeer, L. J., Van Golde, L. M., and Mannaerts, G. P. (1984) Rat liver dihydroxyacetonephosphate acyltransferases and their contribution to glycerolipid synthesis. *J. Biol. Chem.* **259,** 9064–9075
7. Coleman, R. A., and Lee, D. P. (2004) Enzymes of triacylglycerol synthesis and their regulation. *Prog. Lipid Res.* **43,** 134–176
8. Jackowski, S., Wang, J., and Baburina, I. (2000) Activity of the phosphatidylcholine biosynthetic pathway modulates the distribution of fatty acids into glycerolipids in proliferating cells. *Biochim. Biophys. Acta* **1483,** 301–315
9. Leonardi, R., Frank, M. W., Jackson, P. D., Rock, C. O., and Jackowski, S. (2009) Elimination of the CDP-ethanolamine pathway disrupts hepatic lipid homeostasis. *J. Biol. Chem.* **284,** 27077–27089
10. Bagnato, C., and Igal, R. A. (2003) Overexpression of diacylglycerol acyltransferase-1 reduces phospholipid synthesis, proliferation, and invasiveness in simian virus 40-transformed human lung fibroblasts. *J. Biol. Chem.* **278,** 52203–52211
11. Deevska, G. M., Rozenova, K. A., Giltiay, N. V., Chambers, M. A., White, J., Boyanovsky, B. B., Wei, J., Daugherty, A., Smart, E. J., Reid, M. B., Merrill, A. H., Jr, and Nikolova-Karakashian, M. (2009) Acid sphingomyelinase deficiency prevents diet-induced hepatic triacylglycerol accumulation and hyperglycemia in mice. *J. Biol. Chem.* **284,** 8359–8368
12. Osawa, Y., Seki, E., Kodama, Y., Suetsugu, A., Miura, K., Adachi, M., Ito, H., Shiratori, Y., Banno, Y., Olefsky, J. M., Nagaki, M., Moriwaki, H., Brenner, D. A., and Seishima, M. (2011) Acid sphingomyelinase regulates glucose and lipid metabolism in hepatocytes through AKT activation and AMP-activated protein kinase suppression. *FASEB J.* **25,** 1133–1144
13. Merrill, A. H., Jr, Lingrell, S., Wang, E., Nikolova-Karakashian, M., Vales, T. R., and Vance, D. E. (1995) Sphingolipid biosynthesis *de novo* by rat hepatocytes in culture: ceramide and sphingomyelin are associated with, but not required for, very low density lipoprotein secretion. *J. Biol. Chem.* **270,** 13834–13841
14. Schmid, P. C., Spimrova, I., and Schmid, H. H. (1997) Generation and remodeling of highly polyunsaturated molecular species of rat hepatocyte phospholipids. *Lipids* **32,** 1181–1187
15. Mora, G., Scharnewski, M., and Fulda, M. (2012) Neutral lipid metabolism influences phospholipid synthesis and deacylation in *Saccharomyces cerevisiae*. *PLoS One* **7,** e49269
16. Ullman, M. D., and Radin, N. S. (1974) The enzymatic formation of sphingomyelin from ceramide and lecithin in mouse liver. *J. Biol. Chem.* **249,** 1506–1512
17. Nikolova-Karakashian, M. (2000) Assays for the biosynthesis of sphingomyelin and ceramide phosphoethanolamine. *Methods Enzymol.* **311,** 31–42
18. Luberto, C., and Hannun, Y. A. (1998) Sphingomyelin synthase, a potential regulator of intracellular levels of ceramide and diacylglycerol during SV40 transformation: does sphingomyelin synthase account for the putative phosphatidylcholine-specific phospholipase C? *J. Biol. Chem.* **273,** 14550–14559
19. Huitema, K., van den Dikkenberg, J., Brouwers, J. F., and Holthuis, J. C. (2004) Identification of a family of animal sphingomyelin synthases. *EMBO J.* **23,** 33–44

20. Villani, M., Subathra, M., Im, Y. B., Choi, Y., Signorelli, P., Del Poeta, M., and Luberto, C. (2008) Sphingomyelin synthases regulate production of diacylglycerol at the Golgi. *Biochem. J.* **414,** 31–41
21. Adada, M., Luberto, C., and Canals, D. (2016) Inhibitors of the sphingomyelin cycle: Sphingomyelin synthases and sphingomyelinases. *Chem. Phys. Lipids* **197,** 45–59
22. Cornell, R. B., and Northwood, I. C. (2000) Regulation of CTP:phosphocholine cytidylyltransferase by amphitropism and relocalization. *Trends Biochem. Sci.* **25,** 441–447
23. Cases, S., Stone, S. J., Zhou, P., Yen, E., Tow, B., Lardizabal, K. D., Voelker, T., and Farese, R. V. (2001) Cloning of DGAT2, a second mammalian diacylglycerol acyltransferase, and related family members. *J. Biol. Chem.* **276,** 38870–38876
24. Wright, M. M., and McMaster, C. R. (2002) PC and PE synthesis: mixed micellar analysis of the cholinephosphotransferase and ethanolaminephosphotransferase activities of human choline/ethanolamine phosphotransferase 1 (CEPT1). *Lipids* **37,** 663–672
25. Waterman, I. J., Price, N. T., and Zammit, V. A. (2002) Distinct ontogenic patterns of overt and latent DGAT activities of rat liver microsomes. *J. Lipid Res.* **43,** 1555–1562
26. Abo-Hashema, K. A. H., Cake, M. H., Power, G. W., and Clarke, D. (1999) Evidence for triacylglycerol synthesis in the lumen of microsomes via a lipolysis-esterification pathway involving carnitine acyltransferases. *J. Biol. Chem.* **274,** 35577–35582
27. Yen, C. L., Stone, S. J., Koliwad, S., Harris, C., and Farese, R. V., Jr. (2008) Thematic review series: glycerolipids: DGAT enzymes and triacylglycerol biosynthesis. *J. Lipid Res.* **49,** 2283–2301
28. Stone, S. J., Levin, M. C., and Farese, R. V. (2006) Membrane topology and identification of key functional amino acid residues of murine acyl-CoA: diacylglycerol acyltransferase-2. *J. Biol. Chem.* **281,** 40273–40282
29. Fagone, P., and Jackowski, S. (2013) Phosphatidylcholine and the CDP-choline cycle. *Biochim. Biophys. Acta* **1831,** 523–532
30. Coleman, R., and Bell, R. M. (1976) Triacylglycerol synthesis in isolated fat cells: studies on the microsomal diacylglycerol acyltransferase activity using ethanol-dispersed diacylglycerols. *J. Biol. Chem.* **251,** 4537–4543
31. Jacobs, R. L., Devlin, C., Tabas, I., and Vance, D. E. (2004) Targeted deletion of hepatic CTP:phosphocholine cytidylyltransferase α in mice decreases plasma high density and very low density lipoproteins. *J. Biol. Chem.* **279,** 47402–47410
32. Lipsky, N. G., and Pagano, R. E. (1985) A vital stain for the Golgi apparatus. *Science* **228,** 745–747
33. Shayman, J. A., Deshmukh, G. D., Mahdiyoun, S., Thomas, T. P., Wu, D., Barcelon, F. S., and Radin, N. S. (1991) Modulation of renal epithelial cell growth by glucosylceramide: association with protein kinase C, sphingosine, and diacylglycerol. *J. Biol. Chem.* **266,** 22968–22974
34. Rosenwald, A. G., Machamer, C. E., and Pagano, R. E. (1992) Effects of a sphingolipid synthesis inhibitor on membrane transport through the secretory pathway. *Biochemistry* **31,** 3581–3590
35. Li, Z., Fan, Y., Liu, J., Li, Y., Huan, C., Bui, H. H., Kuo, M. S., Park, T. S., Cao, G., and Jiang, X. C. (2012) Impact of sphingomyelin synthase 1 deficiency on sphingolipid metabolism and atherosclerosis in mice. *Arterioscler. Thromb. Vasc. Biol.* **32,** 1577–1584
36. Futerman, A. H., and Pagano, R. E. (1991) Determination of the intracellular sites and topology of glucosylceramide synthesis in rat liver. *Biochem. J.* **280,** 295–302
37. Yamaji, T., and Hanada, K. (2015) Sphingolipid metabolism and interorganellar transport: localization of sphingolipid enzymes and lipid transfer proteins. *Traffic* **16,** 101–122
38. Chaurasia, B., and Summers, S. A. (2015) Ceramides: lipotoxic inducers of metabolic disorders. *Trends Endocrinol. Metab.* **26,** 538–550
39. Chavez, J. A., Knotts, T. A., Wang, L. P., Li, G., Dobrowsky, R. T., Florant, G. L., and Summers, S. A. (2003) A role for ceramide, but not diacylglycerol, in the antagonism of insulin signal transduction by saturated fatty acids. *J. Biol. Chem.* **278,** 10297–10303
40. Bijl, N., Sokolović, M., Vrins, C., Langeveld, M., Moerland, P. D., Ottenhoff, R., van Roomen, C. P., Claessen, N., Boot, R. G., Aten, J., Groen, A. K., Aerts, J. M., and van Eijk, M. (2009) Modulation of glycosphingolipid metabolism significantly improves hepatic insulin sensitivity and reverses hepatic steatosis in mice. *Hepatology* **50,** 1431–1441
41. Mehra, V. C., Jackson, E., Zhang, X. M., Jiang, X. C., Dobrucki, L. W., Yu, J., Bernatchez, P., Sinusas, A. J., Shulman, G. I., Sessa, W. C., Yarovinsky, T. O., and Bender, J. R. (2014) Ceramide-activated phosphatase mediates fatty acid-induced endothelial VEGF resistance and impaired angiogenesis. *Am. J. Pathol.* **184,** 1562–1576
42. Martínez, L., Torres, S., Baulies, A., Alarcón-Vila, C., Elena, M., Fabriàs, G., Casas, J., Caballeria, J., Fernandez-Checa, J. C., and García-Ruiz, C. (2015) Myristic acid potentiates palmitic acid-induced lipotoxicity and steatohepatitis associated with lipodystrophy by sustaning *de novo* ceramide synthesis. *Oncotarget* **6,** 41479–41496
43. Rojas, C., Pan-Castillo, B., Valls, C., Pujadas, G., Garcia-Vallve, S., Arola, L., and Mulero, M. (2014) Resveratrol enhances palmitate-induced ER stress and apoptosis in cancer cells. *PLoS One* **9,** e113929
44. Williams, R. D., Wang, E., and Merrill, A. H., Jr. (1984) Enzymology of long-chain base synthesis by liver: characterization of serine palmitoyltransferase in rat liver microsomes. *Arch. Biochem. Biophys.* **228,** 282–291
45. Kahovcová, J., and Odavić, R. (1969) A simple method for the quantitative analysis of phospholipids separated by thin layer chromatography. *J. Chromatogr.* **40,** 90–96
46. De Clercq, N., Foubert, I., and Dewettinck, K. (2008) Separation and analysis of acylglycerols by chromatographic methods. *Lipid Technol.* **20,** 232–234
47. Sperry, W. M., and Webb, M. (1950) A revision of the Schoenheimer-Sperry method for cholesterol determination. *J. Biol. Chem.* **187,** 97–106
48. Shaner, R. L., Allegood, J. C., Park, H., Wang, E., Kelly, S., Haynes, C. A., Sullards, M. C., and Merrill, A. H., Jr. (2009) Quantitative analysis of sphingolipids for lipidomics using triple quadrupole and quadrupole linear ion trap mass spectrometers. *J. Lipid Res.* **50,** 1692–1707
49. Wurie, H. R., Buckett, L., and Zammit, V. A. (2011) Evidence that diacylglycerol acyltransferase 1 (DGAT1) has dual membrane topology in the endoplasmic reticulum of HepG2 cells. *J. Biol. Chem.* **286,** 36238–36247